Abstract: A passively mode-locked ytterbium-doped large-mode-area photonic crystal fiber oscillator operating in the vicinity of zero cavity dispersion is demonstrated. The self-starting mode-locking operation is achieved by a high contrast saturable absorber mirror. Two mode-locking regimes with opposite signs of net cavity dispersion are investigated. At a net cavity dispersion of –0.0035 ps^2, the fiber laser directly generates 10-nJ laser pulses with an average power of 630 mW at 65.3 MHz repetition rate. The pulses can be dechirped to 78 fs by extracavity dispersion compensation. The pulse energy is scaled up to 18 nJ, yielding an average power of 1.2 W, when the cavity dispersion is set at 0.0035 ps^2. In this regime, the laser output can be extracavity-dechirped to 120 fs. Dynamics of pulse evolution in the fiber laser is illustrated by numerical simulation, which agrees well with experimental results.

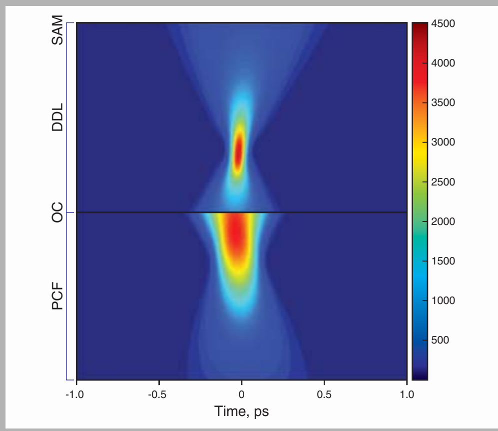

Time-resolved evolution of a light pulse inside a cavity of a mode-locked photonic crystal fiber laser operating in the net negative dispersion regime

Mode-locked Yb-doped large-mode-area photonic crystal fiber laser operating in the vicinity of zero cavity dispersion

Y.-J. Song, [1] *M.-L. Hu,* [1,*] *C.-L. Gu,* [1] *L. Chai,* [1] *C.-Y. Wang,* [1] *and A.M. Zheltikov* [2,*]

[1] Ultrafast Laser Laboratory, Key Laboratory of Optoelectronic Information and Technical Science, College of Precision Instrument and Optoelectronics Engineering, Tianjin University, Tianjin 300072, China
[2] Physics Department, International Laser Center, M.V. Lomonosov Moscow State University, Moscow 119992, Russia

Received: 27 October 2009, Revised: 30 October 2009, Accepted: 2 November 2009
Published online: 14 January 2010

Key words: photonic crystal fiber; femtosecond; fiber laser; mode locking; zero dispersion

PACS: 42.55.Wd, 42.65.Re

1. Introduction

An impressive recent progress in the development of high-energy fiber laser sources of ultrashort pulses [1–4] owes much to in-depth studies of pulse shaping dynamics in fiber lasers, controlled by the balance between the group-velocity dispersion (GVD) and the nonlinear phase shift acquired by light pulses in a fiber. Operating regimes corresponding to different pulse shaping dynamics in mode-locking fiber lasers have been obtained by varying the net cavity dispersion. Fiber lasers with large anomalous cavity dispersion typically function in the soliton mode locking regime, where the pulse energy is severely limited [5]. In the vicinity of zero cavity dispersion, on the other hand, the pulse duration experiences a large change per cavity round trip, which effectively scales down the peak power, thus enabling the generation of higher pulse energies. Pulse energies in excess of 10 nJ have been obtained [6] with fiber lasers either working in the stretched-pulse mode-locking

* Corresponding author: e-mail: huminglie@tju.edu.cn, zheltikov@phys.msu.ru

[7] or self-similar pulse-evolution [8] regime. All normal dispersion lasers support dissipative solitons [9,10], with pulse shaping due to intracavity spectral filtering. Laser pulses with energy of 31 nJ extracavity-compressible to 80 fs have been generated at a repetition rate of 70 MHz in this regime [11].

Specially designed large-mode-area (LMA) photonic crystal fibers (PCFs) [12], which combine reduced optical nonlinearity with pump confinement within a high numerical aperture (NA), become very attractive for scaling up the output average power and pulse energy of ultrafast fiber oscillators. In soliton-like regime, an Yb-doped LMA PCF oscillator with a sigma cavity configuration has been shown to allow a generation of sub-500 fs pulses with 16 nJ pulse energy and 880 mW average power [13]. The environmental stability of the fiber laser is greatly enhanced by using a single-polarization LMA PCF as a gain medium [14]. Such fiber lasers have been used for the creation of compact terahertz sources [15,16]. An LMA PCF amplifier seeded by such fiber oscillator delivering 200 nJ laser pulses with 52 fs pulse duration at a repetition rate of 50 MHz has also been applied for femtosecond laser micromachining [17]. In the all-normal-dispersion regime, pulse energies approaching the microjoule level have been achieved directly from an oscillator based on a rod-type PCF with an effective mode-area of 4000 μm^2 [18]. An Yb-doped LMA Bragg fiber can serve discriminate transverse modes by the photonic band-gap effect, offering much promise for high-energy mode-locking operation [19].

Most of the recent work on LMA PCF lasers is focused on mode locking in the regime of large positive or negative cavity dispersion, where high-energy pulses in the subpicosecond range of pulse widths can be generated. In this paper, we investigate the mode locking of an LMA PCF laser operating in the vicinity of zero cavity dispersion, where the pulse duration can be reduced to several tens of femtoseconds. At a net cavity dispersion of –0.0035 ps^2, the fiber laser directly generates 10-nJ laser pulses with an average power of 630 mW at 65.3 MHz repetition rate. The pulses can be extracavity-dechirped to 78 fs. At a net cavity dispersion of 0.0035 ps^2, the pulse energy is scaled up to 18 nJ, yielding an average power of 1.2 W. In this regime, the pulses can be extracavity-dechirped to 120 fs. We present a numerical model, which directly illustrates the pulse shaping mechanism in our fiber laser and provides an excellent fit for the experimental results.

2. Experimental setup

The experimental setup for the LMA PCF oscillator based on a sigma cavity is illustrated in Fig. 1a. A segment of 0.9 m Yb-doped single polarization LMA PCF (Crystal fiber A/S, Denmark) serves as gain medium. The intrinsically single-mode core has a mode diameter of 29 μm,

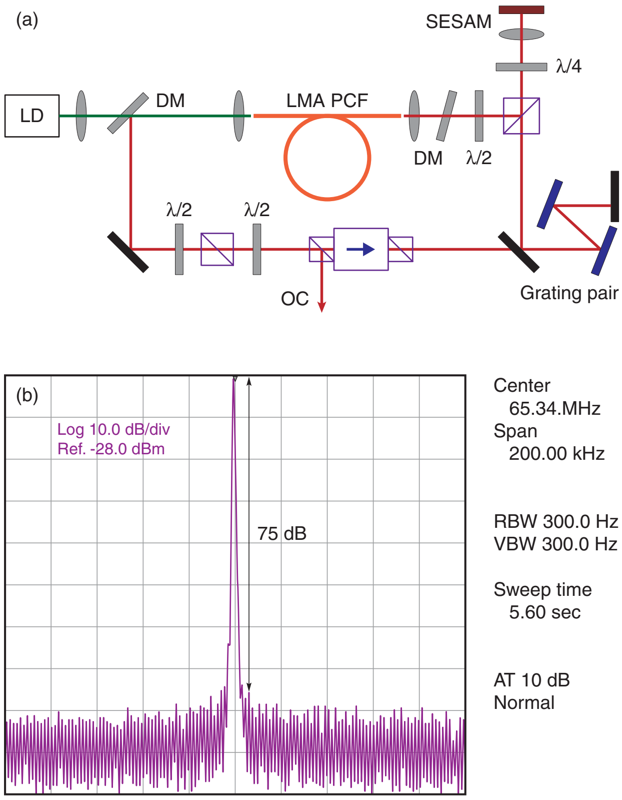

Figure 1 (online color at www.lphys.org) (a) – the experimental setup of the fiber laser. LD: laser diode; DM: dichroic mirror; OC: output coupling; (b) – rf spectrum of the fundamental harmonic recorded with a resolution bandwidth of 300 Hz over 200 kHz frequency span

corresponding to a mode field area of 660 μm^2. The microstructured inner cladding is 200 μm in diameter, and the NA is 0.55 at 950 nm. This structure has a pump light absorption of 10 dB/m. Combined with the LMA structure, index-matched stress applying parts (SAP) are introduced in the photonic-crystal cladding. These induce a birefringence sufficient to split the two polarization states of the weakly guided fundamental mode, serving to maintain a single polarization in the LMA fiber. The bandwidth of single-polarization waveguiding ranges from 1000 to 1100 nm, falling within the gain band of the Yb-doped fiber [20]. The polarization extinction ratio (PER) of the fiber is above 15 dB. Both fiber ends are angle-polished to eliminate parasitic oscillation at a high pump power.

The Yb-doped fiber is cladding-pumped by a fiber-coupled (200 μm, NA=0.22) laser diode emitting at 976 nm. The dichroic mirrors (DMs) are used to separate the pump light from laser radiation. An optical isolator with an isolation rate of 45 dB ensures the unidirectional propagation of light. The rejection port of the isolator combined with a half-wave plate serves as the output coupler. A polarization beam splitter (PBS) together

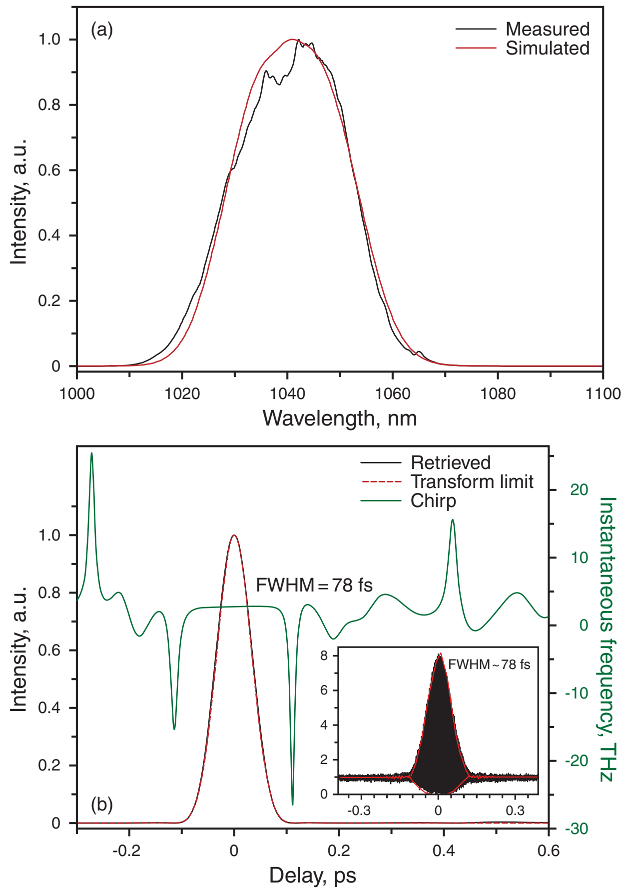

Figure 2 (online color at www.lphys.org) The output characteristics of the fiber laser operating in the net negative dispersion regime. (a) – optical spectrum; (b) – pulse shape as well as instantaneous frequency retrieved by PICASO. The dashed red curve shows the transform limited pulse shape. Inset is the measured interferometric autocorrelation trace of the extracavity dechirped pulses. The red curve shows the simulated envelope of the dechirped pulses

with a half-wave plate is inserted before the isolator in order to enhance polarization discrimination for a high-contrast laser output. A dispersion delay line (DDL) based on a pair of 600-line/mm gratings with a beam incident angle of 35° is used for intracavity dispersion compensation. A grating separation of 13.5 mm can precisely compensate for the normal dispersion of the fiber and optical components inside the cavity, estimated as 0.019 ps^2 at 1040 nm. The total cavity length is about 4.6 m, resulting in a repetition rate of 65.3 MHz. The mode locking is initiated with SESAM (BATOP GmbH, Germany), which has a low-intensity absorption of 65%, modulation depth of 35%, saturation fluence of 20 μJ/cm^2, and relaxation time of about 500 fs.

3. Experimental results and numerical simulations

3.1. Negative cavity dispersion mode-locking regime

A single pulse operation status with slightly negative cavity dispersion is investigated with the separation between the gratings in the DDL equal to 16 mm, and the corresponding net cavity dispersion is –0.0035 ps^2. The fiber laser starts to feature Q-switching at a pump power of 2 W, with transition to mode locking observed at a pump power of 3.4 W. The direct output average power is 630 mW at the pump power of 4.5 W and the output rate of 70%, corresponding to pulse energy of 10 nJ. The measured optical spectrum is shown in Fig. 2a. The spectrum develops a Gaussian shape with an FWHM of 26 nm. The direct output pulse has duration of 375 fs assuming a Gaussian shape. The chirp of the output pulse is compensated with a transmission grating pair based DDL outside the cavity, which induces a reduction of the average power by 30% in the meanwhile. The measured autocorrelation trace of the extracavity-dechirped pulse is shown in the inset of Fig. 2b. The pulse shape and the phase of the dechirped pulses are reconstructed by the phase and intensity from correlation and spectrum only (PICASO) algorithm. The retrieved pulse shape and instantaneous frequency are shown in Fig. 2b. The pulses are nearly transform-limited with the FWHM duration of 78 fs. The corresponding peak power is 89 kW considering the loss in the dechirping stage.

The quality of the pulse train is evaluated by its power spectrum, which is characterized with an rf spectrum analyzer (Agilent 8560EC) via a photodiode with a 200-ps rise time. A typical rf spectrum recorded at the fundamental frequency is shown in the inset of Fig. 1b. The 75-dB signal-to-noise ratio reveals robust mode locking. The calculated rms energy fluctuation is below 0.25%.

Numerical simulations are performed to understand the dynamics of pulse evolution in this mode-locking regime, which has been previously reported in [21,22]. Modeling is performed by solving the nonlinear Schrödinger equation with a standard split-step Fourier algorithm for a pulse passing through a segment of gain fiber having a Lorentzian gain profile with a 50-nm gain bandwidth, an output coupler, a dispersion delay line, and SESAM. Parameters of each intracavity element in our model are identical to those in our experiments. Laser pulse buildup is seeded in our model with white noise.

The simulation gives a direct pulse output with duration of 325 fs and energy of 14 nJ. The pulses can be extracavity-dechirped to 78 fs. The red curve in Fig. 2a and that in the inset of Fig. 2b show the simulated output pulse spectrum and the envelope of the autocorrelation trace of the dechirped pulse shape, respectively. The corresponding intracavity pulse dynamics is shown in Fig. 3. Fig. 3a and Fig. 3b illustrate pulse evolution during one round trip

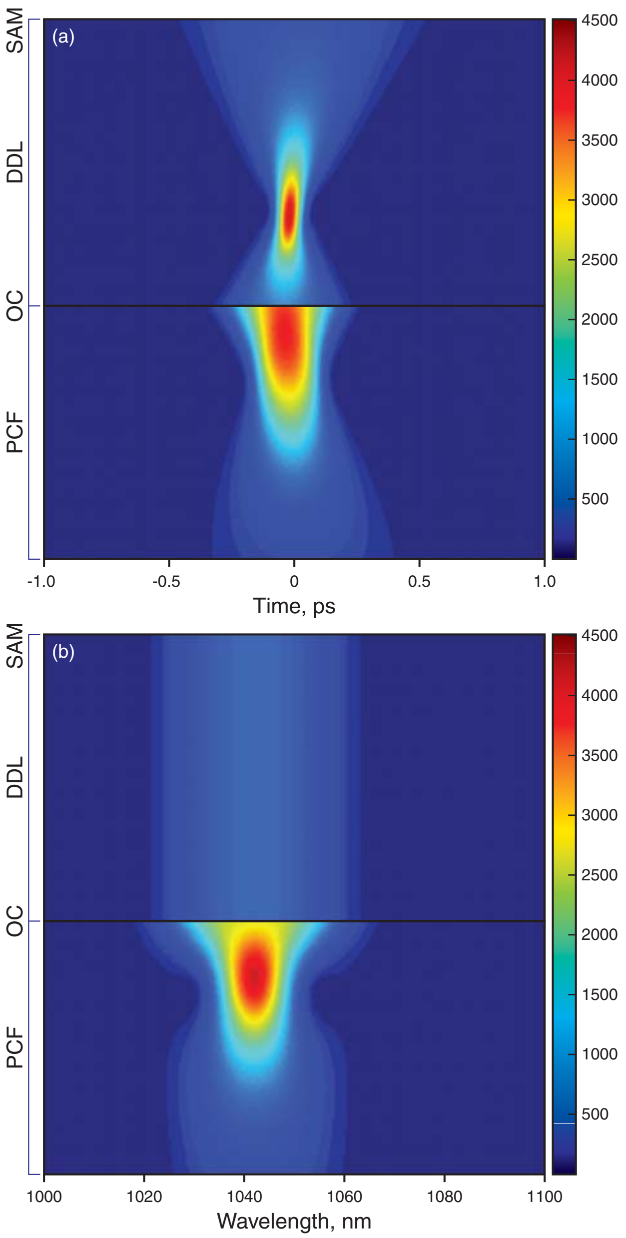

Figure 3 (online color at www.lphys.org) Simulation on the pulse dynamics of the mode-locking fiber laser operating in net negative dispersion regime. (a) – pulse evolution of one round trip in time domain; (b) – pulse evolution of one round trip in frequency domain. (PCF: photonic crystal fiber; OC: output coupler; DDL: dispersion delay line; SAM: semiconductor saturable absorber mirror)

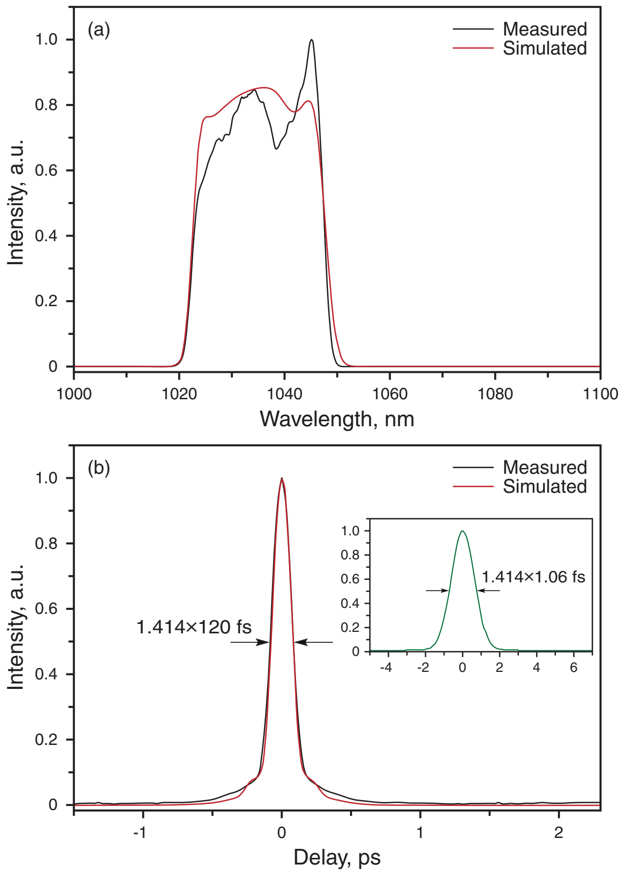

Figure 4 (online color at www.lphys.org) The output characteristics of the fiber laser operating in the net positive dispersion regime. (a) – optical spectrum; (b) – the autocorrelation trace of the extracavity dechirped pulses. Inset, the measured autocorrelation trace of the direct output pulses

in the time and frequency domain, respectively. The pulse duration reaches the transform limit twice per round trip as shown in Fig. 3a, with the stretching ratio equal to 8. The laser operates in a stretched-pulse mode-locking regime. The asymmetric evolution of pulse shape in the time domain is attributed to the asymmetric pulse shape that results from the nonlinear absorption of SESAM. Besides the strong stretching of laser pulses in the time domain, the pulse spectrum also breathes significantly in the PCF with stretching ratio of 2.2, as shown in Fig. 3b, which can be interpreted by the interplay of SPM spectral broadening and gain filtering of limited gain bandwidth. The two effects are exactly balanced at the position inside the fiber corresponds to the minimal spectral width as well as transform-limited pulse duration. The maximal spectral width is achieved at the PCF output.

3.2. Positive cavity dispersion mode-locking regime

By decreasing the separation of grating pair, the net cavity dispersion approaches zero. The output rate has to be reduced in order to keep stable mode-locking operation. In this regime, the fiber laser easily switches to bound state or harmonic mode-locking operation at high pump power.

High energy pulsed operation can be achieved again at a slightly positive net cavity dispersion. The mode-locking regime at a net cavity dispersion of 0.0035 ps^2 is investigated, and the corresponding separation of the grating pair is equal to 11 mm. The direct output average power is 1.2 W at the pump power of 6.4 W and the output rate of 90%. The corresponding pulse energy is 18 nJ. The measured optical spectrum is shown in Fig. 4a. The spectrum develops sharp edges, and has a FWHM of 25 nm. The direct output pulse has duration of 1.06 ps assuming a Gaussian shape, as shown in the inset of Fig. 4b. No satellite-pulses have been detected in a 50 ps scanning range of the autocorrelator. The output pulse is highly chirped, and can be extracavity-compressed to 120 fs, as shown in Fig. 4(b. The peak power of the dechirped pulses is 106 kW considering the loss of DDL.

The pulse dynamics of this mode locking regime is also numerical investigated. The simulation gives a direct pulse output with duration of 0.92 ps and energy of 15 nJ. The pulses can be extracavity-dechirped to 120 fs. The red curve in Fig. 4a and Fig. 4b show the simulated output pulse spectrum and dechirped pulse autocorrelation trace respectively. The asymmetry of the spectrum is also achieved in the numerical simulation, which is due to the nonlinear absorption by SESAM. The sidelobes of the autocorrelation trace indicates the uncompensated nonlinear chirp at the wings of pulses. Fig. 5 reveals the corresponding intracavity pulse evolution dynamics. As shown in Fig. 5a, the pulse broadens and compresses itself monotonically in the fiber and in the DDL, respectively, with the stretching ratio equals to 3.5. The spectrum keeps a steep-edged shape and show neglectable stretching in the round trip evolution.

The laser has shown characteristics of self-similar operation in this mode-locking regime, where the pulse duration evolves monotonously in the active fiber, and the pulse spectrum approaches a parabolic shape. The finite gain bandwidth of the long active fiber ultimately limits the self-similar evolution of laser pulses in the cavity, and also prevents further scaling of the pulse energy.

In summary, the pulse dynamics shows significant difference for a LMA PCF laser operating in the vicinity of zero cavity dispersion with contrary signs. In the stretched pulse mode locking regime which corresponds to slightly negative cavity dispersion, soliton formation dominates pulse shaping dynamics. Sub-100 fs pulse duration is achieved due to soliton compression effect. On the other hand, the pulse energy is limited by soliton break-up. In the positive dispersion regime, soliton formation is effectively avoided, and the pulse energy can be greatly scaled up, while the pulse duration can't be compressed down accordingly. Additionally, Gain filtering of the long fiber restricts the pulse shortening in both regimes. Pulses with higher energy and shorter duration can be obtained by adding a long piece of passive LMA PCF for pulse stretching and by reducing the active fiber length as long as the highly doped LMA PCF is available.

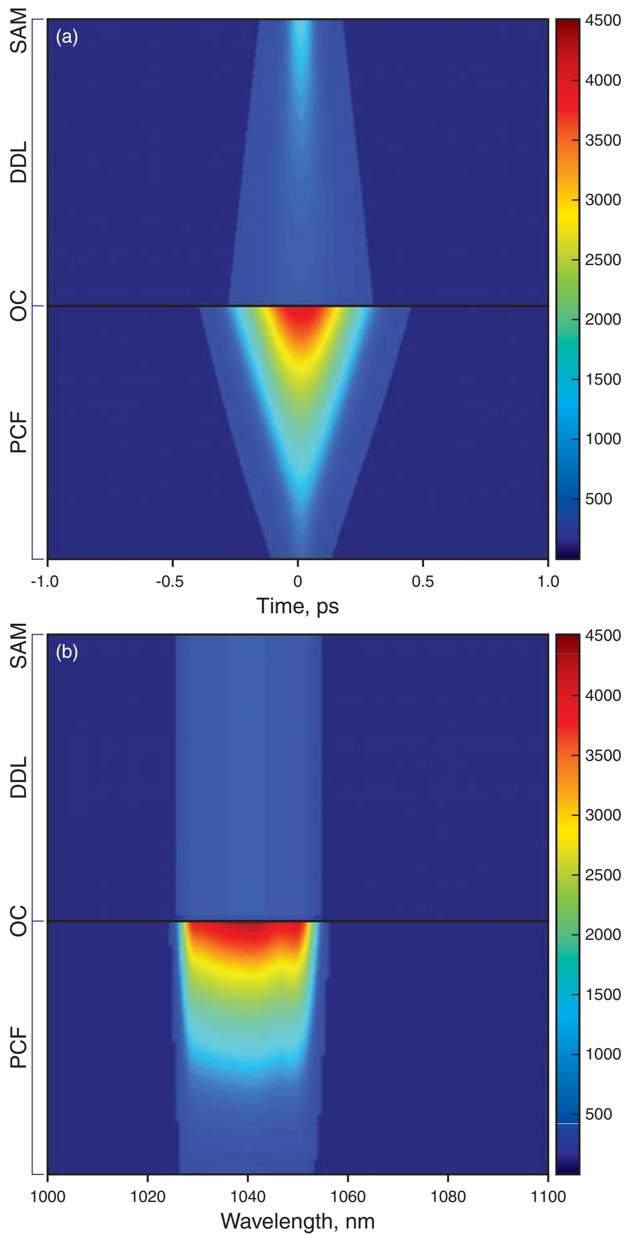

Figure 5 (online color at www.lphys.org) Simulation on the pulse dynamics of the mode-locking fiber laser operating in net positive dispersion regime. (a) – pulse evolution of one round trip in time domain; (b) – pulse evolution of one round trip in frequency domain. (PCF: photonic crystal fiber; OC: output coupler; DDL: dispersion delay line; SAM: semiconductor saturable absorber mirror)

4. Conclusion

In conclusion, an Yb-doped single polarization LMA PCF laser mode-locked in the vicinity of zero cavity dispersion is investigated. The self-starting mode-locking operation is achieved by high contrast saturable absorber. At a net cavity dispersion of –0.0035 ps^2, the fiber laser operates in the stretched pulse regime and directly generates 10-nJ laser pulses with an average power of 630 mW at 65.3 MHz repetition rate. The pulses can be dechirped to 78 fs by extracavity dispersion compensation. When the net cavity dispersion is set at 0.0035 ps^2, the fiber laser shows characteristics of self-similar operation, where the pulse energy is scaled up to 18 nJ, yielding an average power of 1.2 W, and the pulse can be extracavity-dechirped to 120 fs. The numerical simulation illustrates the pulse evolution in this LMA PCF laser operating in such mode-locking regimes.

Acknowledgements This work is supported by the State Key Development Program for Basic Research of China (Grants No. 2010CB327604 and No. 2006CB806002), the National High Technology Research and Development Program of China (Grant No. 2007AA03Z447), the National Natural Science Foundation of China (Grants No. 60678012 and No. 60838004), the 111 Project (Grant No. B07014), the Key Project of Chinese Ministry of Education (Grant No. 108032), the FANEDD (Grant No. 2007B34), the NCET (NCET-07-0597), the Russian Foundation for Basic Research (Projects No. 08-02-91756, No. 08-02-92226, No. 08-02-92009, No. 09-02-12359, and No. 09-02-12373), and the Federal Program of the Russian Ministry of Education and Science (Contracts No. 1130 and No. 02.740.11.0223).

References

[1] J. Limpert, F. Roser, T. Schreiber, and A. Tunnermann, IEEE J. Sel. Top. Quantum Electron. **12**, 233 (2006).
[2] M.E. Fermann and I. Hartl, Laser Phys. Lett. **6**, 11 (2009).
[3] C. Fortier, B. Kibler, J. Fatome, C. Finot, S. Pitois, and G. Millot, Laser Phys. Lett. **5**, 817 (2008).
[4] H. Luo, D.Y. Tang, G.Q. Xie, H.J. Zhang, L.J. Qin, H.H. Yu, and L.J. Qian, Laser Phys. Lett. **5**, 651 (2008).
[5] K. Tamura, L.E. Nelson, H.A. Haus, and E.P. Ippen, Appl. Phys. Lett. **64**, 149 (1994).
[6] J.R. Buckley, F.W. Wise, F.Ö. Ilday, and T. Sosnowski, Opt. Lett. **30**, 1888 (2005).
[7] K. Tamura, E.P. Ippen, and H.A. Haus, Appl. Phys. Lett. **67**, 158 (1995).
[8] F.Ö. Ilday, J.R. Buckley, W.G. Clark, and F.W. Wise, Phys. Rev. Lett. **92**, 213902 (2004).
[9] A. Chong, J. Buckley, W. Renninger, and F. Wise, Opt. Express **14**, 10095 (2006).
[10] W.H. Renninger, A. Chong, and F.W. Wise, Phys. Rev. A **77**, 023814 (2008).
[11] K. Kieu, W.H. Renninger, A. Chong, and F.W. Wise, Opt. Lett. **34**, 593 (2009).
[12] J. Limpert, O. Schmidt, J. Rothhardt, F. Röser, T. Schreiber, A. Tünnermann, S. Ermeneux, P. Yvernault, and F. Salin, Opt. Express **14**, 2715 (2006).
[13] B. Ortaç, J. Limpert, and A. Tünnermann, Opt. Lett. **32**, 2149 (2007).
[14] B. Ortaç, C. Lecaplain, A. Hideur, T. Schreiber, J. Limpert, and A. Tünnermann, Opt. Express **16**, 2122 (2008).
[15] Y.-J. Song, M.-L. Hu, C.-L. Wang, Z. Tian, Q.-R. Xing, L. Chai, and C.-Y. Wang, IEEE Photon. Tech. Lett. **20**, 1088 (2008).
[16] G. Matthäus, B. Ortaç, J. Limpert, S. Nolte, R. Hohmuth, M. Voitsch, W. Richter, B. Pradarutti, and A. Tünnermann, Appl. Phys. Lett. **93**, 261105 (2008).
[17] B.-W. Liu, M.-L. Hu, X.-H. Fang, Y.-Z. Wu, Y.-J. Song, L. Chai, C.-Y. Wang, and A.M. Zheltikov, Laser Phys. Lett. **6**, 44 (2009).
[18] B. Ortaç, M. Baumgartl, J. Limpert, and A. Tünnermann, Opt. Lett. **34**, 1585 (2009).
[19] C. Lecaplain, A. Hideur, S. Février, and P. Roy, Opt. Lett. **34**, 2879 (2009).
[20] T. Schreiber, F. Röser, O. Schmidt, J. Limpert, R. Iliew, F. Lederer, A. Petersson, C. Jacobsen, K. Hansen, J. Broeng, and A. Tünnermann, Opt. Express **13**, 7621 (2005).
[21] R. Herda and O.G. Okhotnikov, Appl. Opt. **47**, 1182 (2008).
[22] T. Schreiber, B. Ortaç, J. Limpert, and A. Tünnermann, Opt. Express **15**, 8252 (2007).